

KEK-preprint-94-162
 NWU-HEP 94-07
 DPNU-94-59
 TIT-HPE-94-013
 TUAT-HEP 94-07
 OCU-HEP 94-07
 PU-94-692
 INS-REP 1077
 KOBE-HEP 94-06

Measurement of inclusive particle spectra and test of MLLA prediction in e^+e^- annihilation at $\sqrt{s}=58\text{GeV}$

(TOPAZ collaboration)

R.Itoh^a, M.Yamauchi^a, A.Yamaguchi^b K.Abe^c, T.Abe^c, I.Adachi^a, K.Adachi^b, M.Aoki^c, M.Aoki^d, S.Awa^b, K.Emi^e, R.Emomoto^a, H.Fujii^a, K.Fujii^a, T.Fujii^f, J.Fujimoto^a, K.Fujita^g, N.Fujiwara^b, H.Hayashii^b, B.Howell^h, N.Iida^b, Y.Inoue^g, H.Iwasaki^a, M.Iwasaki^b, K.Kaneyuki^d, R.Kajikawa^c, S.Katoⁱ, S.Kawabata^a, H.Kichimi^a, M.Kobayashi^a, D.Koltick^h, I.Levine^h, S.Minami^d, K.Miyabayashi^c, A.Miyamoto^a, K.Muramatsu^b, K.Nagai^j, K.Nakabayashi^c, E.Nakano^c, O.Nitoh^e, S.Noguchi^b, A.Ochi^d, F.Ochiai^k, N.Ohishi^c, Y.Ohnishi^c, Y.Ohshima^d, H.Okunoⁱ, T.Okusawa^g, T.Shinohara^e, A.Sugiyama^c, S.Suzuki^c, S.Suzuki^d, K.Takahashi^e, T.Takahashi^g, T.Tanimori^d, T.Tauchi^a, Y.Teramoto^g, N.Toomi^b, T.Tsukamoto^a, O.Tsumura^e, S.Uno^a, T.Watanabe^d, Y.Watanabe^d and A.Yamamoto^a

(a) KEK, National Laboratory for High Energy Physics, Ibaraki-ken 305, Japan

(b) Department of Physics, Nara Women's University, Nara 630, Japan

(c) Department of Physics, Nagoya University, Nagoya 464, Japan

(d) Department of Physics, Tokyo Institute of Technology, Tokyo 152, Japan

(e) Department of Applied Physics, Tokyo Univ. of Agriculture and Technology, Tokyo 184, Japan

(f) Department of Physics, University of Tokyo, Tokyo 113, Japan

(g) Department of Physics, Osaka City University, Osaka 558, Japan

(h) Department of Physics, Purdue University, West Lafayette, IN 47907, USA

(i) Institute for Nuclear Study, University of Tokyo, Tanashi, Tokyo 188, Japan

(j) The Graduate School of Science and Technology, Kobe University, Kobe 657, Japan

(k) Faculty of Liberal Arts, Tezukayama University, Nara 631, Japan

Abstract

Inclusive momentum spectra are measured for all charged particles and for each of π^\pm , K^\pm , $K^0/\overline{K^0}$, and p/\overline{p} in hadronic events produced via e^+e^- annihilation at $\sqrt{s}=58\text{GeV}$. The measured spectra are compared with QCD predictions based on the modified leading log approximation(MLLA). The MLLA model reproduces the measured spectra well. The energy dependence of the peak positions of the spectra is studied by comparing the measurements with those at other energies. The energy dependence is also well described by the MLLA model.

1 Introduction

The LLA (leading log approximation) parton shower model well reproduces the various distributions of observables for hadronic final states of e^+e^- collisions, when the ‘‘coherence’’ effect of soft gluons is taken into account. Several Monte Carlo programs were written based on this scheme (JETSET63[1], for example) and were used in various experiments to study QCD. However, since the coherence effect is the consequence of higher order corrections, the effect could only be inserted by hand in the LLA scheme in these Monte Carlo programs.

On the other hand, even in low Q^2 region, the momentum spectrum of gluons in the parton shower process can be analytically calculated using the modified leading log approximation(MLLA)[2]. The coherence effect is taken into account in MLLA by consistently importing a part of next-to-leading order corrections. The distribution of the particle spectra is expressed as a function of two parameters, $Y=\log(\frac{E\Theta}{Q_0})$ and $\lambda=\log(\frac{Q_0}{\Lambda})$:

$$x_p \overline{D}_q^g(x, Y, \lambda) = \frac{4C_F(Y + \lambda)}{bB(B + 1)} \int_{\epsilon+i\infty}^{\epsilon-i\infty} \frac{d\omega}{2\pi i} x_p^{-\omega} \Phi(-A + B + 1, B + 2, -\omega(Y + \lambda)) \times \frac{\Gamma(A)}{\Gamma(B)} (\omega\lambda)^B \Psi(A, B + 1, \omega\lambda) \quad (1)$$

Here x_p is the momentum of a particle normalized by the beam energy $E = \sqrt{s}/2$, Θ is the opening angle of the jet cone, and $C_F=\frac{4}{3}$, $b=\frac{23}{3}$, $A=\frac{12}{b\omega}$ and $B=\frac{307}{27b}$ for five quark flavors, respectively. The two functions, Φ and Ψ , are two solutions of the confluent hyper-geometric equation. The quantities Λ and Q_0 are the QCD scale parameter and the energy cut-off of the parton evolution, respectively.

This calculation predicts depletion of soft partons as a consequence of the destructive interference of soft gluons. This depletion shows up clearly in eq. 1 when written as a function of $\xi = \ln(1/x_p)$. This function has a maximum at a certain ξ value and decreases in the larger ξ region. The coherence effect reduces the available phase space in this region and therefore the effect can be studied by comparing the measured inclusive cross section with this calculation.

However, since this expression is calculated for partons, it cannot be compared directly with the measurement unless the distribution at the level of final state hadrons is ensured to be similar to that of partons. The concept of Local Parton Hadron Duality (LPHD) dictates that the distribution of the final state hadrons

is closely related to that of partons[3]. The conversion of partons into hadrons, which occurs at low virtuality scale, includes only small momentum transfer, and hence leaves the distribution essentially unchanged. In this article we compare the calculated parton spectrum (eq. 1) directly with the measured hadron spectrum assuming LPHD.

The Q_0 , which was primarily introduced to regularize collinear singularity, gives a cut-off on parton energies. Therefore, the value of Q_0 should be close to the mass of the particle being considered[4], while Λ should be common to all the particle species. These dependences can be experimentally tested by measuring the values of Q_0 and Λ for various particle species.

The momentum spectrum might still be distorted by fragmentations and decays in spite of LPHD. This complication can be avoided partially when the energy evolution of the distribution is considered. The peak position of the distribution (eq. 1) is given using the limiting spectra calculation in which Λ is assumed to be equal to Q_0 [2]:

$$\xi_{max} = \frac{1}{2}Y + B\sqrt{\frac{b}{16N_c}Y - \frac{bB^2}{16N_c}} \quad (2)$$

where N_c is the number of colors ($= 3$). This should be compared with the variation as $\xi_{max} \sim Y$ expected from phase space consideration alone.

2 Event Selection

The data used in this analysis are accumulated by the TOPAZ detector at the TRISTAN e^+e^- collider at center-of-mass energies between 52.0 and 61.4 GeV. The average energy is 58.0 GeV, and the total integrated luminosity is 113.7/pb.

Details of the TOPAZ detector is described elsewhere[5]. In this analysis, the data from a Time Projection Chamber (TPC) is mainly used for tracking and dE/dx measurement for charged particles[6]. The trigger condition relevant to this analysis is the track trigger which requires two or more charged tracks in the fiducial volume of the TPC, and the energy trigger which requires 4 GeV or more energy deposit in the barrel lead glass calorimeter. The event trigger is generated by a logical OR of those two, and the trigger efficiency for multihadronic events is practically 100%.

Out of the triggered events, multihadronic events are selected by the following conditions; (a) five or more charged tracks having transverse momenta with

respect to the beam axis larger than $0.15 \text{ GeV}/c$ are originating from the interaction point with the angle larger than 37° with respect to the beam axis, (b) total visible energy is larger than $1/2$ of the center-of-mass energy, and (c) momentum imbalance along the beam direction is smaller than 0.4 . By these conditions, the event selection efficiency is estimated to be 67.1% with a background contamination of less than 2.0% . Two-photon processes and $\tau^+\tau^-$ productions are the main sources of the background. In addition to these cuts, the jet axis is required to have an angle larger than 40° with respect to the beam axis to ensure that the event is well contained in the detector acceptance. Applying these criteria, 11247 events remain to be used in the analysis.

3 Particle Identification and Measurement of Cross section

The particle species π^\pm , K^\pm and p/\bar{p} are identified by measuring the dE/dx of tracks detected in TPC. The detail of the particle identification technique is described in ref.[7]. The typical resolution of the dE/dx measurement for minimum ionizing pions is 4.6% . Fig. 1 shows dE/dx distribution as a function of the track momentum for a part of the event sample.

The cross section is calculated from the number of tracks in each momentum slice. In the low momentum region, the number of tracks for each particle species are directly obtained by counting the number of tracks in each dE/dx band. The dE/dx bands are, however, not well separated in the higher momentum region. To extract the number of each particle species in this region, the dE/dx distribution in a momentum slice is fitted with a superposition of four Gaussians corresponding to e^\pm , π^\pm 's, K^\pm 's and p/\bar{p} in each momentum slice. The widths and the centers of the Gaussians are determined from the measurement for Bhabha events and cosmic ray μ 's. Only the normalizations of the Gaussians are the free parameters of the fit. A typical fit to the dE/dx distribution is shown in Fig. 2. Because of a hardware calibration problem of the TPC, the dE/dx resolution is time dependent. Therefore the data sample is divided into two groups and the procedure to count the number of tracks of each particle species is done separately for these two groups.

K_s 's are identified by searching for their daughter charged pion pairs in TPC.

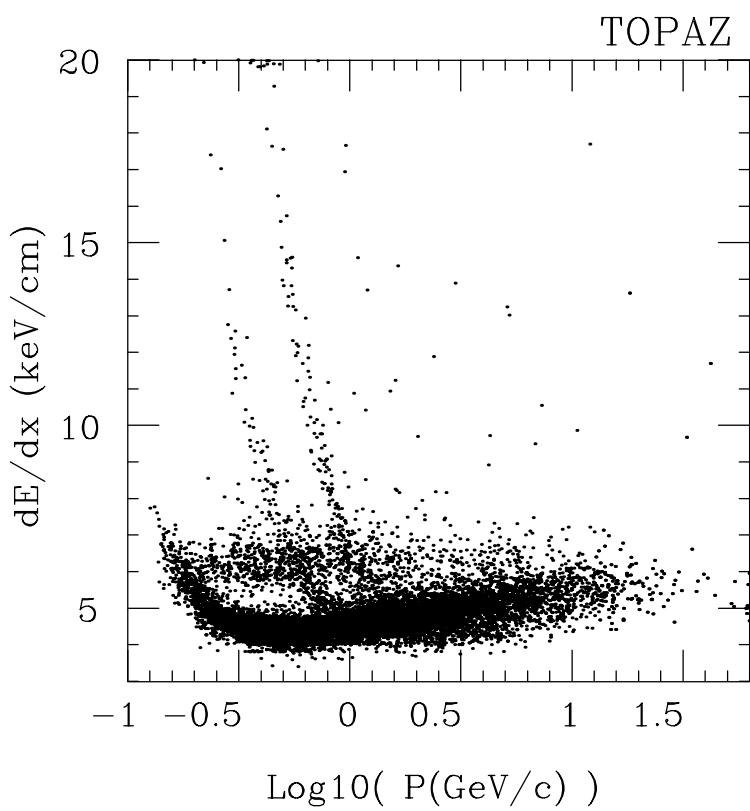


Figure 1: dE/dx distribution as a function of track momentum measured by TOPAZ-TPC.

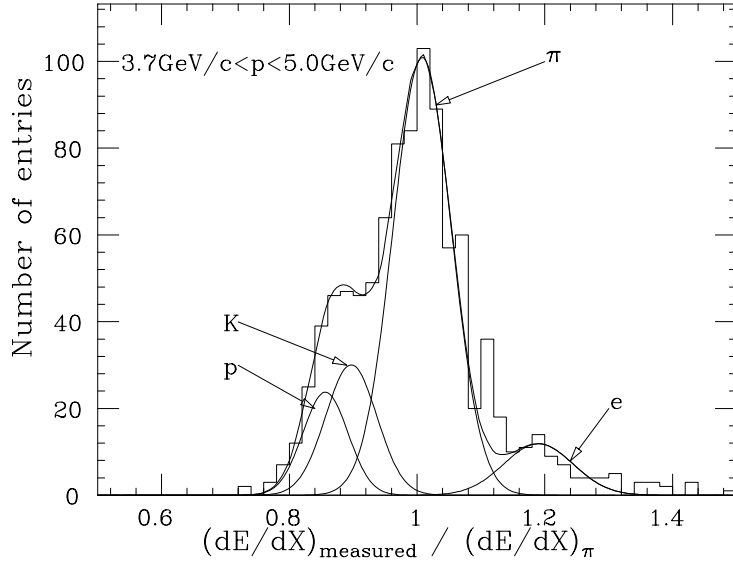


Figure 2: A typical fit to dE/dx distribution in a momentum bin. The distribution is fitted by four Gaussians corresponding to e^\pm , π^\pm , K^\pm and p/\bar{p} .

A pair of tracks must satisfy following conditions to be identified as a K_s : a) the distance of the closest approach of the two tracks is less than 0.8cm; b) the distance from the interaction point to the decay vertex is longer than 2.0cm where the decay vertex is defined as the center of the closest approach of two tracks; c) the angle formed by the vector from the interaction point to the decay vertex and the momentum sum of the two tracks at the decay vertex is less than 8 degrees if the position of decay vertex is longer than 6.0 cm; or c') the closest distance from the vector sum to the interaction point is less than 0.6 cm if the decay length is shorter than 6.0 cm; d) the closest approach of one of the tracks to the interaction point is more than 0.5cm if the momentum sum of the tracks is less than $2\text{GeV}/c$; e) tracks are identified as π^\pm by the dE/dx measurement in the TPC; and f) the tracks are not from the gamma conversion.

For each of track pairs remained after these selections, the invariant mass is calculated assuming the tracks are charged pions. Fig. 3 shows the mass distribution for the reconstructed K_s 's. The distribution is fitted by a sum of a Gaussian

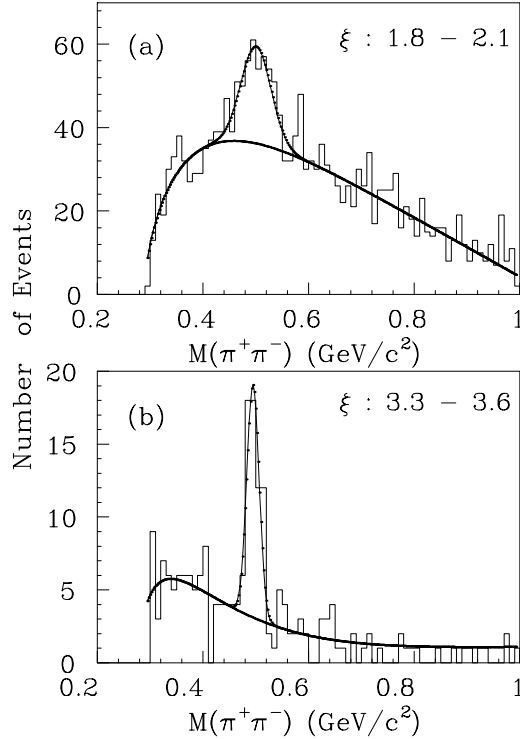


Figure 3: Reconstructed mass distributions of K_s in two different momentum bins:
 (a) $1.8 < \xi < 2.1$, (b) $3.3 < \xi < 3.6$

and a background function (exponential + polynomial) and the number of reconstructed K_s 's is obtained to be 771 ± 61 . In the same way, the numbers of these K_s 's are counted for each momentum slice.

The inclusive cross section, $1/\sigma_{had} d\sigma/dx_p$ is then calculated from the number of particles observed in each momentum slice using following formula:

$$\frac{1}{\sigma_{had}} \frac{d\sigma}{dx_i} = A(x_i) \frac{1}{\Delta x_i} \frac{N_{obs}(x_i)}{N_{had}}, \quad (3)$$

where x_i is the i 'th slice of the momentum fraction, σ_{had} is the total hadronic cross section, Δx_i is the width of the slice, N_{had} is the number of hadronic events in the event sample, and $N_{obs}(x_i)$ is the number of particles counted in the slice, respectively. $A(x_i)$ is the factor to correct the counted number for the effects

of detector acceptance and initial state radiation. $A(x_i)$ is calculated for each momentum slice separately with the Monte Carlo simulation as

$$A(x_i) = \frac{N_{gen}(x_i)}{N_{gen}^{total}} / \frac{N_{sim}(x_i)}{N_{sim}^{total}} \quad (4)$$

where $N_{gen}(x_i)$ is the generated number of particles in the slice x_i without including the effects of the detector acceptance and the initial state radiation. N_{gen}^{total} is the corresponding total number of generated events. $N_{sim}(x_i)$ is the number of detected particles in the slice x_i generated with the effects of detector acceptance and initial state radiation, and N_{sim}^{total} is the corresponding total number of generated events. The JETSET6.3[1] and 7.3[8] Monte Carlo programs are used to obtain these numbers combined with the TOPAZ detector simulation program. As for K_s , to convert the counted number to the cross section of $K^0/\overline{K^0}$, $A(x_i)$ is multiplied by 2.

The cross sections are measured as a function of ξ . The measured cross section for all charged particles is shown in Table 1. Table 2 shows the cross sections measured for each of π^\pm , K^\pm , p/\overline{p} , while that for $K^0/\overline{K^0}$ is shown in Table 3.

The systematic error in the measurement is estimated by considering following sources. One is the systematic ambiguity in the acceptance correction. This is studied by varying the fragmentation parameters in the Monte Carlo programs and by turning on and off the energy loss and the nuclear interaction effects in the detector simulation program. The ambiguity is estimated to be 2% for all charged particles while 3% for π^\pm , K^\pm and p/\overline{p} . For π^\pm , K^\pm and p/\overline{p} , the ambiguity in the dE/dx curve as a function of momentum used to extract numbers of each particle species is also a source of the systematic error. This is estimated to be 5% for π^\pm and 10% for K^\pm and p/\overline{p} .

4 Comparison with MLLA prediction

The measured particle spectra are then compared directly with the MLLA predictions by assuming LPHD. Since the Λ and Q_0 in the MLLA calculation are unknown, their values are determined by fitting the MLLA formula of the cross section to the data. Fig. 4 shows the measured cross section for all charged particles as a function of ξ together with the result of the best fit shown in the solid line. As seen from Fig. 4, the fitted MLLA calculation well reproduces the measured cross section.

| $\xi = \ln(1/x_p)$ | $1/\sigma_{tot} d\sigma/d\xi$ |
|--------------------|-------------------------------|
| 0.7 | 0.287 ± 0.015 |
| 0.9 | 0.656 ± 0.018 |
| 1.1 | 0.942 ± 0.024 |
| 1.3 | 1.313 ± 0.031 |
| 1.5 | 1.783 ± 0.041 |
| 1.7 | 2.455 ± 0.055 |
| 1.9 | 3.116 ± 0.067 |
| 2.1 | 3.547 ± 0.076 |
| 2.3 | 4.182 ± 0.089 |
| 2.5 | 4.380 ± 0.093 |
| 2.7 | 4.877 ± 0.103 |
| 2.9 | 5.089 ± 0.107 |
| 3.1 | 5.674 ± 0.119 |
| 3.3 | 5.705 ± 0.120 |
| 3.5 | 5.673 ± 0.119 |
| 3.7 | 5.406 ± 0.114 |
| 3.9 | 5.135 ± 0.109 |
| 4.1 | 4.564 ± 0.098 |
| 4.3 | 4.037 ± 0.087 |
| 4.5 | 3.265 ± 0.071 |
| 4.7 | 2.498 ± 0.055 |
| 4.9 | 1.637 ± 0.046 |

Table 1: Measured cross section for all charged particles as a function of ξ . Errors include both of statistical and systematic errors.

| $\xi = \ln(1/x_p)$ | $1/\sigma_{tot} d\sigma/d\xi$ | | |
|--------------------|-------------------------------|-----------------|-----------------|
| | π^\pm | K^\pm | p/\bar{p} |
| 1.32 | 1.07 \pm 0.12 | 0.41 \pm 0.08 | 0.17 \pm 0.04 |
| 1.62 | 1.50 \pm 0.14 | 0.61 \pm 0.10 | 0.25 \pm 0.05 |
| 1.92 | 2.24 \pm 0.21 | 0.63 \pm 0.10 | 0.23 \pm 0.04 |
| 2.22 | 2.75 \pm 0.23 | - | - |
| 2.47 | 3.25 \pm 0.27 | - | - |
| 2.62 | 3.75 \pm 0.42 | 0.75 \pm 0.19 | 0.30 \pm 0.21 |
| 2.77 | 3.95 \pm 0.64 | 0.69 \pm 0.16 | 0.33 \pm 0.22 |
| 2.98 | 3.84 \pm 0.80 | - | - |
| 3.22 | - | - | - |
| 3.41 | 4.75 \pm 0.50 | 0.51 \pm 0.08 | 0.22 \pm 0.04 |
| 3.51 | 4.86 \pm 0.46 | 0.39 \pm 0.06 | 0.20 \pm 0.03 |
| 3.61 | 4.79 \pm 0.37 | 0.44 \pm 0.06 | 0.21 \pm 0.03 |
| 3.77 | 4.53 \pm 0.37 | 0.48 \pm 0.06 | 0.13 \pm 0.02 |
| 3.96 | 4.18 \pm 0.34 | 0.29 \pm 0.04 | - |
| 4.14 | 3.82 \pm 0.36 | 0.24 \pm 0.03 | - |
| 4.42 | 3.27 \pm 0.28 | 0.12 \pm 0.02 | - |
| 4.71 | 2.27 \pm 0.18 | - | - |
| 4.83 | 1.94 \pm 0.17 | - | - |

Table 2: Measured cross sections for π^\pm , K^\pm and p/\bar{p} as functions of ξ . Special non-uniform binning of ξ is used to optimize the particle identification by the dE/dx measurement. Errors include both of statistical and systematic errors.

| $\xi = \ln(1/x_p)$ | $1/\sigma_{tot} d\sigma(K_s)/d\xi$ |
|--------------------|------------------------------------|
| 1.80 | 0.58 ± 0.10 |
| 2.25 | 0.65 ± 0.12 |
| 2.55 | 0.68 ± 0.10 |
| 2.85 | 0.61 ± 0.09 |
| 3.15 | 0.62 ± 0.09 |
| 3.45 | 0.49 ± 0.09 |
| 3.80 | - |
| 4.25 | - |
| 4.05 | 0.23 ± 0.04 |

Table 3: Measured cross section for K^0/\bar{K}^0 as a function of ξ . Errors are statistical only.

Fig. 5 shows the cross sections measured for π^\pm , K^\pm , K^0/\bar{K}^0 and p/\bar{p} with the fitted MLLA calculations. Also shown are the measurements by PEP4/TPC[9] at $\sqrt{s} = 29\text{GeV}$ for π^\pm , K^\pm , and p/\bar{p} . These measurements are also fitted by the MLLA calculations. The fit is performed in the range where the numerical calculation of the MLLA function is reliable. The range is typically $1.0 < \xi < 4.0$. The measured cross sections are well reproduced by MLLA. The figure demonstrates the energy evolution of the peak position of the spectra: the peak position in ξ becomes larger in TOPAZ measurements at $\sqrt{s} = 58\text{GeV}$ than those of PEP4/TPC at $\sqrt{s} = 29\text{GeV}$ regardless of particle species. This is also predicted by the MLLA calculation. The detail of the study of the evolution of the peak position is described in the next section.

Tables 4 and 5 summarize the obtained values of Λ and Q_0 . Two different fits are performed: one is to determine both of Λ and Q_0 from the fit, and the other is to determine Q_0 from the fit with Λ fixed at 200 MeV. In both cases, the value of Q_0 becomes larger for heavier particles. Meanwhile, in the first case, the determined value of Λ stays at relatively lower values (100-300 MeV). This result gives a strong support to the MLLA + LPHD conjecture.

| | TOPAZ(58GeV) | | PEP4(29GeV) | |
|----------------------|-----------------|--------------|-----------------|---------------|
| Free fit | Λ (MeV) | Q_0 (MeV) | Λ (MeV) | Q_0 (MeV) |
| all charged | 291 \pm 10 | 375 \pm 8 | - | - |
| π^\pm | 281 \pm 20 | 339 \pm 25 | 270 \pm 7 | 250 \pm 7 |
| K^\pm | 118 \pm 68 | 575 \pm 80 | 243 \pm 74 | 531 \pm 80 |
| $K^0/\overline{K^0}$ | 185 \pm 19 | 649 \pm 76 | - | - |
| p/\overline{p} | 143 \pm 81 | 657 \pm 90 | 356 \pm 105 | 531 \pm 100 |

Table 4: Λ and Q_0 for each of particle species determined from the fits with both Λ and Q_0 as free parameters.

| | TOPAZ(58GeV) | PEP4(29GeV) |
|----------------------|---------------|--------------|
| $\Lambda = 200$ MeV | Q_0 (MeV) | Q_0 (MeV) |
| all charged | 297 \pm 12 | - |
| π^\pm | 275 \pm 12 | 217 \pm 6 |
| K^\pm | 588 \pm 44 | 514 \pm 45 |
| $K^0/\overline{K^0}$ | 663 \pm 110 | - |
| p/\overline{p} | 627 \pm 92 | 390 \pm 50 |

Table 5: Q_0 for each of particle species determined by the fits with Λ fixed at 200MeV.

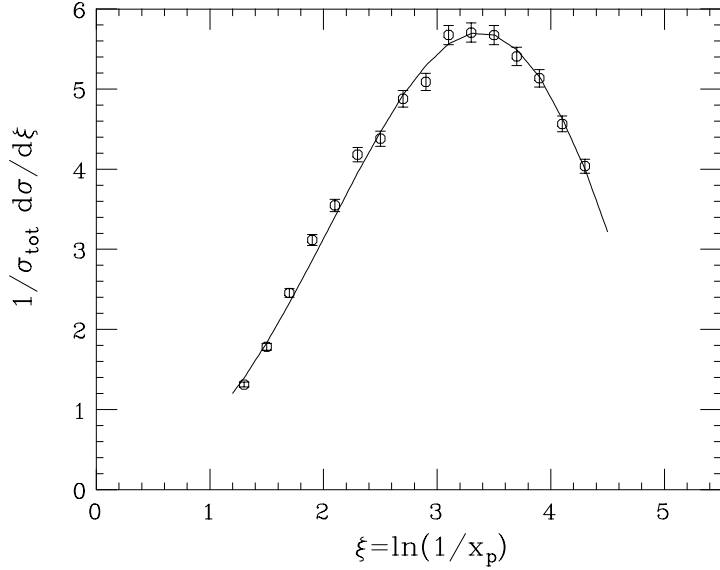


Figure 4: The cross section measured for all charged particles as a function of $\xi = \ln(1/x_p)$. Solid curve shows the fitted MLLA calculation.

5 The Energy Evolution of ξ Distribution

The energy evolution of the peak positions in ξ is studied by comparing the measurements at $\sqrt{s}=29\text{GeV}$ (PEP4/TPC), 58GeV (TOPAZ) and 91GeV (ALEPH)[10] as a part of the PTA project[11]. Table 6 shows the result. The peak positions and their errors are estimated using the fitted MLLA functions for PEP4 and TOPAZ measurements. The MLLA predictions using the limiting spectra calculation (eq. 2) with $\Lambda = 200\text{MeV}$ are also shown. As seen, the peak positions for light particles (all charged particles and π^\pm) agree with the limiting spectra calculation. The peak positions become smaller for heavier particles regardless of the energy scale.

From eq. 2, the MLLA prediction of peak position can be approximated in the linear form $a \ln E + b$ where a to be 0.5. If the gluon coherence effect is not taken into account (phase space only), a should become 1.0. To obtain the value of a from the measured peak positions, a linear fit is performed to the peak positions

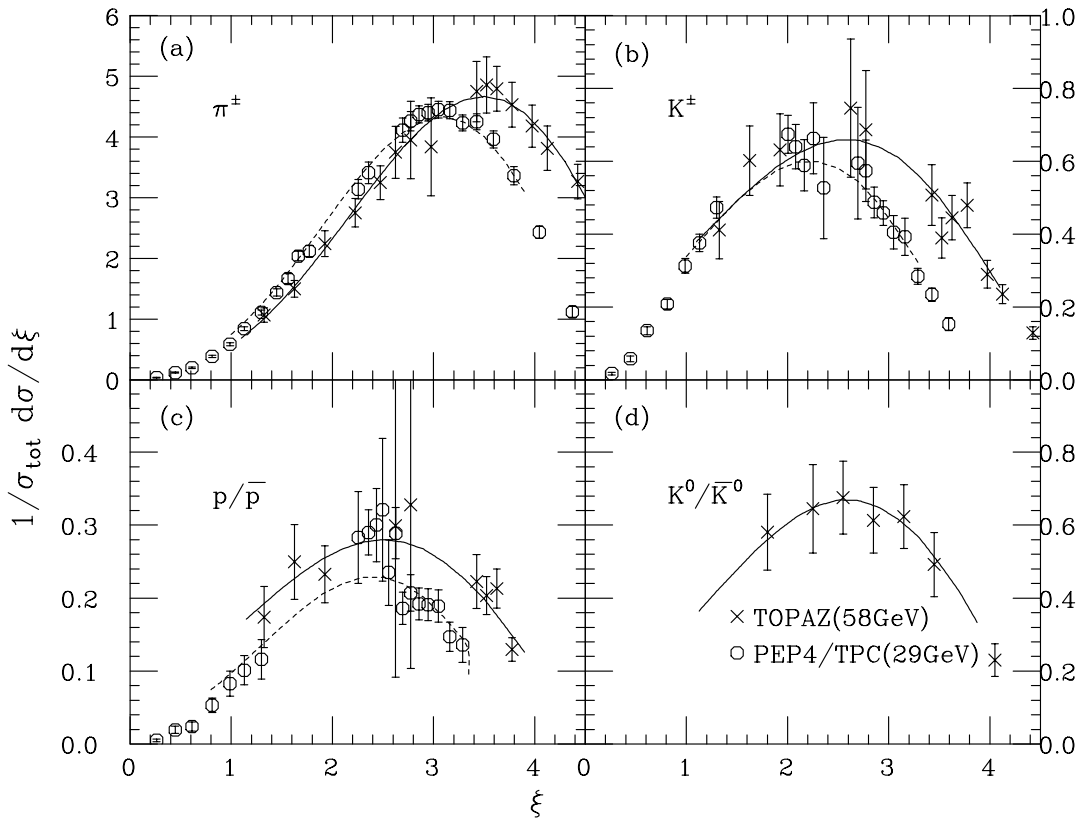


Figure 5: The cross sections measured for (a) π^\pm , (b) K^\pm , (c) p/\bar{p} and (d) K^0/\bar{K}^0 . Both of TOPAZ and PEP4/TPC measurements are plotted with MLLA fits (Solid curve:TOPAZ, Dashed curve:PEP4).

| | PEP4/TPC(29GeV) | TOPAZ(58GeV) | ALEPH(91GeV) |
|-----------------------------------|-----------------|-----------------|-----------------|
| all charged | - | 3.30 ± 0.05 | 3.61 ± 0.01 |
| π^\pm | 3.10 ± 0.12 | 3.48 ± 0.18 | 3.81 ± 0.02 |
| K^\pm | 2.30 ± 0.20 | 2.56 ± 0.29 | 2.63 ± 0.04 |
| K^0/\bar{K}^0 | - | 2.90 ± 0.24 | 2.88 ± 0.03 |
| p/\bar{p} | 2.30 ± 0.20 | 2.50 ± 0.29 | 3.00 ± 0.09 |
| MLLA($\Lambda = 200\text{MeV}$) | 3.02 | 3.46 | 3.74 |

Table 6: The energy evolution of the peak positions in ξ . Also shown are predictions obtained using the limiting spectra calculation of MLLA.

as a function of \sqrt{s} for all charged particles measured by TASSO[12], TOPAZ, and ALEPH as shown in Fig. 6. From the fit, the value of a is obtained to be 0.54 ± 0.05 . A similar fit is also done to the peak positions for charged pions (TASSO, PEP4/TPC, TOPAZ and ALEPH) and a is measured to be 0.58 ± 0.04 . These values are consistent with the MLLA predictions.

6 Summary

The inclusive cross sections are measured as a function of $\xi = \ln(1/x_p)$ for all charged particles and for each of π^\pm , K^\pm , p/\bar{p} and K^0/\bar{K}^0 in the hadronic events taken at $\sqrt{s}=58\text{GeV}$. The cross sections were compared with the MLLA calculation assuming LPHD. The MLLA formula describes the observed distributions very well for all particle species over the wide momentum range.

By this comparison, Q_0 and Λ in the MLLA expression are determined for each particle species. The determined Q_0 for each of the particle species is close to the mass of the particle, while the Λ is almost constant for these particles. The Q_0 values are also determined with Λ fixed at 200MeV. The obtained Q_0 also coincides with the mass of each particle. The same analysis is carried out for the measurements at $\sqrt{s} = 29\text{GeV}$ by PEP4/TPC and similar tendency is observed. These results show that the momentum distribution of particles is identical to that of partons at the end-point of the parton shower evolution independently of the energy scale. This supports the MLLA + LPHD conjecture.

The energy evolution of the peak position in $d\sigma/d\xi$ is studied by comparing

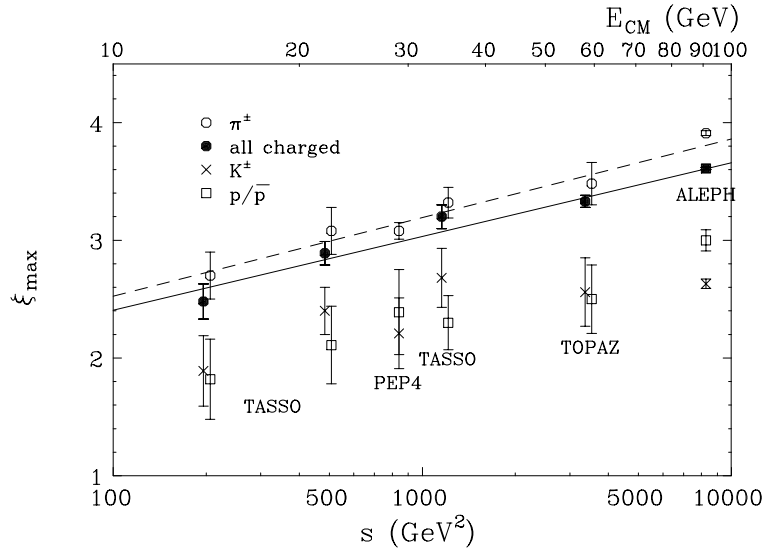


Figure 6: The peak position in ξ as a function of the square of the center-of-mass energy. Solid line shows the linear fit to the peak positions of charged particles while dashed line to those of charged pions.

our data with the measurements by PEP4/TPC and ALEPH. The measured peak positions of light particles are well reproduced by the limiting spectra calculation. The measured peak positions are fitted to a linear function of log of the beam energy with the measurements at other energies. The obtained slope of the linear function is consistent with the MLLA prediction, while it excludes models without the gluon coherence effect.

References

- [1] T.Sjöstrand, Comp. Phys. Comm **39** (1986) 347; T.Sjöstrand and M.Bengtsson, Comp. Phys. Comm **43** (1987) 367.
- [2] A. Basseto et al., Phys. Rep. **100** (1983) 201; Yu. L. Dokshitzer et al., Rev. of Mod. Phys., **60** (1988) 373; Yu. L. Dokshitzer et al., in Perturbative QCD, ed. A. H. Mueller (World Scientific, Singapore, 1989) 241; V. A. Khoze, NATO ASI: Z0 Physics 1990 (1990) 419; Yu. L. Dokshitzer, V. A. Khoze and S. I. Troyan, LU TP 91-12 (1991).
- [3] Ya. I. Azimov et al., Z. Phys. **C27** (1985) 65.
- [4] Ya. I. Azimov et al., Z. Phys. **C31** (1986) 213; Ya. I. Azimov et al., Z. Phys. **C27** (1985) 65.
- [5] R. Enomoto et al., Nucl. Instrum. Methods **A269** (1988) 507; T.Tsukamoto, M.Yamauchi and R.Enomoto, Nucl. Instrum. Methods **A297** (1990) 148; A. Imanishi et al., Nucl. Instrum. Methods **A269** (1988) 513; T. Kamae et al., Nucl. Instrum. Methods **A252** (1986) 423; A. Yamamoto et al., Jpn. J. Appl. Phys. Lett. **25** (1986) L440; S. Kawabata et al., Nucl. Instrum. Methods **A270** (1988) 11; J. Fujimoto et al., Nucl. Instrum. Methods **A256** (1987) 449; S. Noguchi et al., Nucl. Instrum. Methods **A271** (1988) 404; K. Fujii et al., Nucl. Instrum. Methods **A264** (1988) 297.
- [6] T. Kamae et al., Nucl. Instrum. Methods **A252** (1986) 423.
- [7] R.Itoh, Doctoral Thesis, Univ. of Tokyo (1988), unpublished.
- [8] T.Sjöstrand, “PYTHIA 5.6 AND JETSET 7.3: PHYSICS AND MANUAL”, CERN-TH-6488-92 (1992).
- [9] H.Aihara et al. (TPC/Two Gamma Collab.), LBL-23737 (1988).
- [10] R.J. Hemingway, “Spectra of identified particles”, presented at XXVII International Conference on High Energy Physics, Glasgow (1994).
- [11] PTA collaboration was formed to study the energy dependence of QCD. This is the joint effort of PEP4/TPC, TOPAZ and ALEPH collaborations.
- [12] M. Althoff et al. (TASSO Collab.), Z.Phys. **C22** (1984) 307.

This figure "fig1-1.png" is available in "png" format from:

<http://arxiv.org/ps/hep-ex/9412015v1>

This figure "fig1-2.png" is available in "png" format from:

<http://arxiv.org/ps/hep-ex/9412015v1>

This figure "fig1-3.png" is available in "png" format from:

<http://arxiv.org/ps/hep-ex/9412015v1>

This figure "fig1-4.png" is available in "png" format from:

<http://arxiv.org/ps/hep-ex/9412015v1>

This figure "fig1-5.png" is available in "png" format from:

<http://arxiv.org/ps/hep-ex/9412015v1>

This figure "fig1-6.png" is available in "png" format from:

<http://arxiv.org/ps/hep-ex/9412015v1>